



Application of Joint Inversion of Resistivity and Seismic Refraction Tomography to Investigate the Cause of Structural Failure in an Office Complex

Collins C. Chiemeké

Physics Department Federal University Otuoke, Yenagoa, Bayelsa State, Nigeria

Abstract Structural failure of office complex floor has recently occurred in isolated places at different time within the offices of Federal University Otuoke. Speculation off the possible causes has been attributed to poor construction work, while others have associated it to the underlying geology; a few attributed the cause to the recent earth tremors that were noticed in different part of the country. It has caused both panic and psychological fear within the University community each time it occurred. Hence the aim of this research work is to investigate the possible cause of the structural failure and proffer a lasting solution, using geophysical method. In a bid to achieve this, resistivity tomography and seismic refraction tomography were used to carry out this investigation. The results of the resistivity and seismic refraction tomography survey, couple with the geologic log for both profile revealed that, apart from the superficial surface sand filling, that the area under investigation is predominantly clay, down to a depth of 9 m. However, this is underlain by a layer of saturated sand at a depth of 10 m. Profile 2 positioned beside the office complex where structural failure occurred, show regions of low resistivity and velocity encompassed by region of high resistivity and velocity. It was discovered that the structural failures were engender by uneven contraction of the different types of clay, which triggered a compressional force effect, that lead to the fracturing and compression of the floor tiles. It was recommended that before putting up any structure in similar geologic environment, that adequate geophysical survey has to be carried out to ascertain the existing lithology and establish the subsurface geometry. Secondly the area should be excavated to a depth of 1 m and before unvaryingly filled with sand material. It was also advised that when replacing the broken tiles with new tiles, a gap of 1.5 cm should be left in between tiles, filled with compressible material to give room for expansion and prevent future reoccurrence.

Keywords Structural failure; resistivity; seismic refraction; tomography; Clay; Sand; Hand Auger

1. Introduction

Massive structural failure of office complex floor has recently (as at January and February, 2017) occurred in several isolated places within the premises of Federal University Otuoke. Some of the pictures taken immediately after the occurrence of the structural failure are shown in figure 1 and 2.

The cause of the structural failure was speculative, a group attributed it to poor construction work, while some other groups attributed it to the underlying geology, and a few attributed it to the recent earth tremor being experienced in the different part of the country. Each time it occurred, it sparks both panic and psychological fear for the occupant of the particular office within the University community. Hence the need to investigate the cause of the sudden structural failure and possibly offer solution to the problem became paramount. To achieve this series of questions were raised, if it was poor construction, the gradual compression effect noticed in figure 1 for a 1 cm thick strong ceramic tiles could not be explained. If the structural failure was due to underlying geology, the first suspect is clay, but clay would rather contract at the peak of dry season when the structural failure occurred, than expand to cause such a compression. If the failure is as a result of the tremor being



experienced within that period in some part of the country, it would have been wide ranged than being localized in a single office. However, the only thing that could provide the clue to what could have possibly caused the structural failure is to investigate the underlying geology on which the building is resting on.



Figure 1: Structural failure of office floor, (16th, February, 2017) showing crack lines and displacement (a) Front view (b) Back view



Figure 2: Structural failure of office floor, (16th, January, 2017) showing crack lines and displacement (a) Front view (b) Side view

Three methods were selected for the purpose of this investigation. The first method is resistivity tomography, this method was selected to measure the resistivity distribution within the subsurface, that could possibly provide clue to the surface lithology and geometry. The second method which is seismic refraction tomography was selected to also complement and confirm the structural geometry and lithology by taking advantage of seismic velocity distribution. The third method which is drilling with Hand Auger is to have insight into the underlying geology. Two profile points were selected for this survey. The first profile was located on the part of the building where structural failure has not been experienced, while the profile 2 is located very close to the foundation of the offices that has experienced structural failure. Previous works done by other researchers were also reviewed. [1] has earlier stated that “Several attempts made to proffer solution to structural failure excluded geophysical investigations, as general opinion did not support subsurface geology as being responsible”. [1], correlated 2D resistivity imaging and seismic refraction tomography to study the depositional history of an environment. “When the ground around your home or property becomes very dry the ground shrinks, and your foundation shifts” [6]. “Cracked tile flooring is a difficult problem. In most cases, the problem



is not with the tiles but with the materials below the tile, and because the cause is hidden below, you cannot easily investigate this cause” [9].

The instruments used for resistivity tomography survey include; SAS 1000 Tetrameter, Four steel unpolarizable electrodes, four reels of cables, and Power Battery (Fig. 3). The instruments used for the seismic refraction tomography include; 12 Channel Digital Seismograph, Reel of cable with takeout point, Trigger Coil, 13 Geophones, Sledge Hammer, Base Plate, and Power Battery (Fig. 4).



Figure 3: Resistivity Tomography Equipment

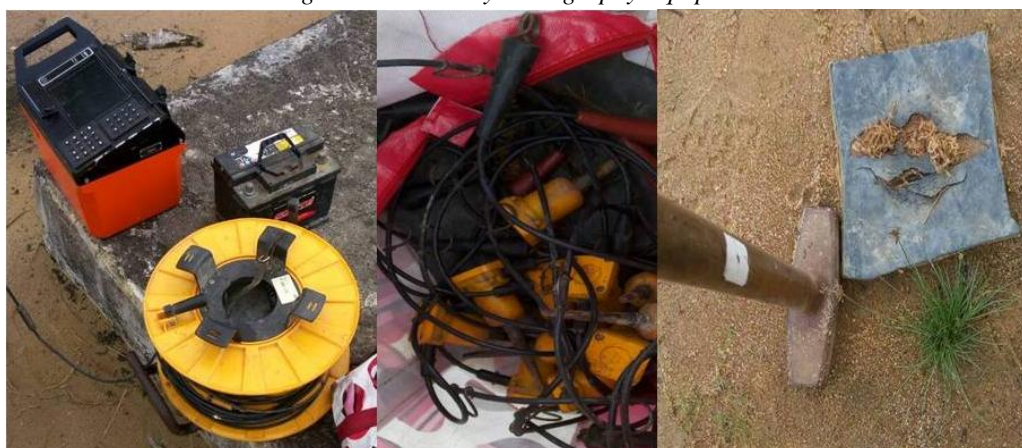


Figure 4: Seismic Refraction Tomography Equipment

2. Location of the study area

The study area is Otuoke and its Environ, which is located in the Oil rich Niger Delta of Bayelsa state, South-South Nigeria. The average elevation of Otuoke and its environ is 18 m above mean sea level [3]. The study location is bounded by $4^{\circ} 47' 30.20N''$, $6^{\circ} 19' 14.89E''$; $4^{\circ} 47' 31.19N''$, $6^{\circ} 19' 15.86E''$; $4^{\circ} 47' 30.35N''$, $6^{\circ} 19' 15.69E''$; $4^{\circ} 47' 31.26N''$, $6^{\circ} 19' 16.51E''$ as indicated with the pin-out on image map of figure 5.

3. Geology of the study area

“The study area is Otuoke and its environs in Bayelsa state, within the fresh water and meander belt geomorphic unit of the Niger Delta”, [10]. The Formation of the present Niger Delta started during Early Paleocene as a result of the built up of fine grained sediments eroded and transported to the area by the River Niger and its tributaries. The regional geology of the Niger Delta consists of three lithostratigraphic units; Akata, Agbada and Benin Formations, overlain by various types of Quaternary Deposits [14], [16], [8]. These Quaternary Sediments, according to [11] are largely alluvial and hydromorphic soils and lacustrine sediments of Pleistocene age. “The result of the overburden thickness analysis and the velocity distribution at the surface down to a depth

of 5 m, has revealed that Otuoke and Its Environs is characterized with regions of low velocities and regions of high velocities that falls within the range of sandy clay” [4].



Figure 5: Image Map of the Survey area indicating the profile lines, their start and end coordinate. Adapted from [5].

4. Data acquisition

The data acquisition for the Wenner Schlumberger array resistivity survey started by placing the 18 electrodes for profile 1, and 16 electrodes for profile 2, in a straight line. The electrodes were planted at an interval of 2.5 m for the two profiles. Profile 1 has a total spread length of 0 to 42.5 m, while profile 2 has a total spread length of 0 to 37.5 m. During the data acquisition, four electrodes were selected each time, and the corresponding resistance value was measured. At the first measurement the distance between the 4 electrodes was 2.5 m. At the second layer measurement the distance between the two potential electrodes did not change, but the distance between the first current electrode and the first potential electrode was increased to 5 m, also the distance between the second potential electrode and the last current electrode was increased to 5 m. Making it a 5 m, 2.5 m, 5 m spread, the measurement of the resistance values using this array was continued along the profile. Other array distances used include 7.5 m, 2.5 m, 7.5 m; 10 m, 2.5 m, 10 m, etc. The measured resistance values at each data point were recorded for both profiles for onward processing.

The data acquisition for seismic refraction tomography started by planting the receivers in a straight line. The 12 geophones were planted at an interval of 2.5 m along the profile line. An offset distance of 7.5 m for profile 1, with an offset distance of 5m for profile 2 were used before the first geophone and after the last geophone to acquire the seismic data. When all the necessary connection was completed, shots were deployed at each shot point, at each receiver station, at an interval of 2.5 m. A total number of 18 shots points were used to acquire the data in profile 1 with a spread length of 0 to 42.5 m, and a total number of 16 shots points were used to acquire the data in profile 2, with a spread length of 0 to 37.5 m. After 5 stacks of shots with a sledge hammer at each shot point, the shot was advance 2.5 m to the next shot point, where a stack of 5 shots were repeated. The generated seismograms at every shot point were recorded for onward processing in the geophysical laboratory.

Four points were identified along the profile lines for drilling base on the results of the generated models for resistivity and seismic tomography. Point 1 and point 2, are 17.5 m and 31.5 m along profile 1, and, point 3 and



point 4 were located 10.0 m and 28.5 m respectively along profile 2. The points were drilled down to a depth of 3 m each, by turning the Hand Auger instrument. The soil samples were collected at different depths which were used to generate a geologic log for each point drilled.

5. Data Processing

The processing of the resistivity data started with the conversion of the data measured in resistance in Ω , to apparent resistivity in Ωm using the Wenner Schlumberger geometric factor. The geometry of the electrode spacing was included with the converted apparent resistivity on the same file. The file was imported into the geophysical software used for the data processing. The software calculated the true resistivity and depth from the input apparent resistivity using a Jacobian matrix calculation with forward modeling procedures and robust least squares inversion algorithm. It basically does this by iteratively comparing the observed data and the calculated model to generate the true model, until a good fit is achieved.

Data Processing of the acquired seismic data started by importing the raw seismic data into dedicated software used for the processing. The imported seismic data was edited for possible wrong geometry. The bandpass filter was applied using an upper cut off frequency of 150 Hz and a lower cut off frequency of 50 Hz to suppress high frequency signal and very low frequency signals, like the surface waves. The gain filter was applied to reduce the effect geometrical spreading. The first arrival travel time was picked by selecting the first kick on the wiggle traces. The inversion process was carried out on the picks times, to generate the initial model for the first and second layers. Ray-tracing which is necessary to determine the ray-path that can be used to model the velocity profile was carried out. After which the initial generated model was iteratively inverted to generate tomography model by incorporating static correction information directly into the inversion routine.

6. Result and Discussion

The result of the resistivity tomography models are shown in figure 6. It represents a model of the distribution of true resistivity within the subsurface. It is displayed in shades of rainbow colour for easy of interpretation. The housing unit under investigation is indicated with a bolded line in the form of a rectangle, while the drilled points are indicated with inverted triangles. The length of profile 1 is, 47.5 m, and probe down to a depth of 7 m, while the length of profile 2 is 37.5 m and probe down to a depth of 6 m. The resistivity model of Profile 1 which was located in offices where structural failure has not been reported showed a general increase of resistivity with depth. The model resistivity for profile 1 ranges from 0.291 Ωm at the surface to 814 Ωm . The resistivity model for profile 2 which lies beside the offices that has experienced structural failure ranges between 0.0181 Ωm to 609 Ωm . These resistivity values for profile 1 and 2 falls within the standard resistivity range of clay and sand (Standard resistivity of clay and sand ranges from 1 Ωm to 1000 Ωm (Clay 1 to 100 Ωm , sand 60 to 1000 Ωm) after [7], 100 to 200 Ωm for compacted Clay, 50 to 500 Ωm for Clayely Sand, 200 to 300 Ωm for Siliceous Sand, 1 to 30 Ωm for swampy soil, after [15]). A clear analysis of profile 1 resistivity tomography model indicate that it is made up of clay material, with resistivity range of 1 Ωm to 150 Ωm within the upper 3.5 m. The layering structure prevalent in profile 1 shows absence of resistivity anisotropy, meaning to a great extent a low resistivity layer is underlain by a high resistivity layer that stretch reasonably across the profile.

Profile 2 resistivity tomography model did not depict a section of layering structure, but is characterize with a lot of resistivity anisotropy with a section of high resistivity underlain by low resistivity, and area of low resistivity being flanked by regions of high resistivity. The range of resistivity which is between 0.0181 Ωm to 609 Ωm , shows that regions with resistivity values of 0.02 Ωm to 31 Ωm is made up of swampy soil that comes in the form of clay. This can be noticed at a distance of 10 m along the profile. This is flanked by region of high resistivity, with resistivity range of 50 Ωm to 500 Ωm , which can be categorized as region of compacted Clayely Sand. Emplaced also within this region is area of high resistivity with resistivity range of 600 Ωm to 800 Ωm that could be categorized as sandy clay. A distance of 28.5 m along profile 2 also depicts region of low resistivity that is flanked by regions of high resistivity. The offices where these structural failures occurred are located within these regions where low resistivity is flanked by high resistivity, which is at a distance of 10 m and 28.5 m respectively. A close examination of the resistivity model of profile 2, gives us a better clue of what was responsible for the generation of the compressional force that led to the cracking of the office floor, noticed



in figure 2. During the wet season, the clay materials absorb water and swells. However During the dry season it losses water and contract. In November 2016, the rain came to an abrupt end, plunging Bayelsa into a period of dry condition which was contrary to the usual norm were rainfall is still intermittent in Bayelsa state throughout the dry season. This must have resulted to the swampy clay materials located at a distance of 10 m and 28.5 m along profile 2, contracting more than the adjoining sandy clay, which trigger the compressional force that is convergent on the swampy clay, and lead to the structural failures noticed in figure 1 and 2.

Base on the results of the resistivity and seismic tomography modeling, couple with proximity to the points of occurrence of the structural failure, four points were selected for drilling with a Hand Augar instrument shown in figure 7. This technique was included to get a firsthand knowledge of the underlying geology in the area under investigation. The drilled points in figure 6 and 8 are indicated with inverted triangles and pin-out respectively. The coordinates of the drilled points are: Point 1, 4° 47'30.61''N, 6° 19' 15.30''E; Point 2, 4° 47' 30.93''N, 6° 19' 15.61''E; Point 3, 4° 47' 30.60''N, 6° 19' 15.93''E; Point 4, 4° 47' 31.0''N, 6° 19' 16.35''E. Each point was drilled down to a depth of 3 m. The soil samples collected from each drilled points are shown in figure 9. Each of the drilled point was logged, and the logs are shown in figure 10 to 13. The soil samples and the logs of the drilled points revealed a layer of "sand fill" at the surface down to a depth 0.9 m for point 1, 0.95 m for point 2, 0.85 m for point 3, and 0.78 m for point 4. The sand filled layer at the surface is the aftermath of the sand filling that was carried out, before erecting the building. A close examination shows that they are intermingled with clay to an extent. Immediately beneath the sand layer is the silty clay, which connotes a scene where humus materials were laying on top of the clay before the sand filling. At this layer you have large portion of clay with silty grains. The thickness of these layers is 0.7 m at point 1, 0.7 m at point 2, 0.63 m at point 3, 0.62 m at point 4. Beneath this layer, is still a layer of clay mixed with reddish iron content. The depth to this layer is 1.6 m for point 1, 1.65 m for point 2, 1.48 m for point 3, 1.42 m for point 4. The rest log details are shown in figure 10 to 13. The result of this drilling method has revealed that the area under investigation is predominantly clay and sand.

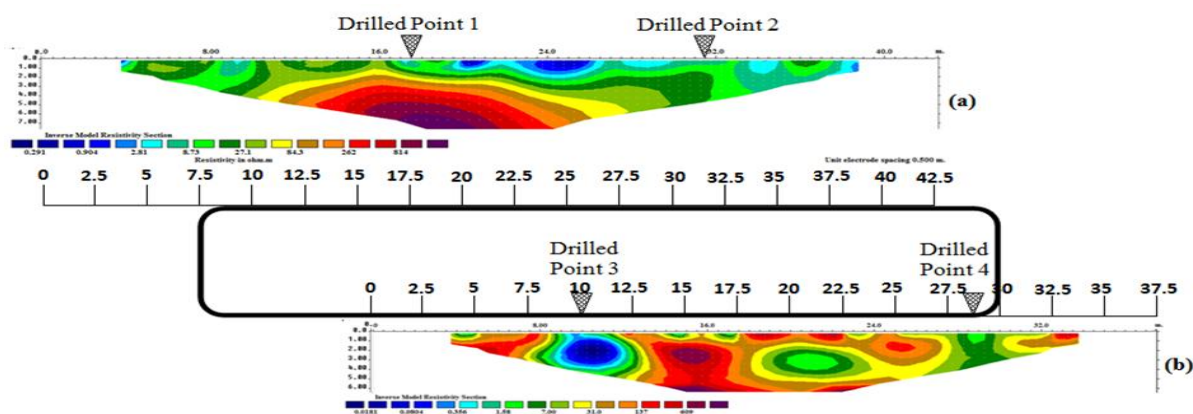


Figure 6: 2D Resistivity tomography models indicating profile lines around housing unit under investigation, (a) Profile 1 (b) Profile 2



Figure 7: Hand Auger instrument used for the drilling process

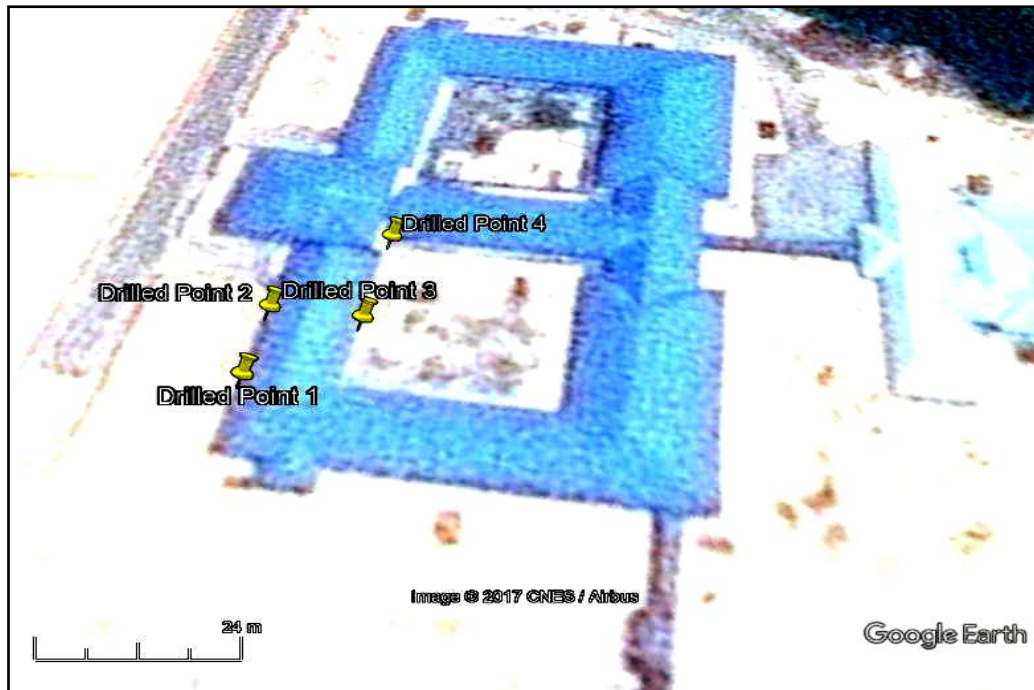


Figure 8: Image map showing the drilled points with Pin-outs. Adapted from [5]

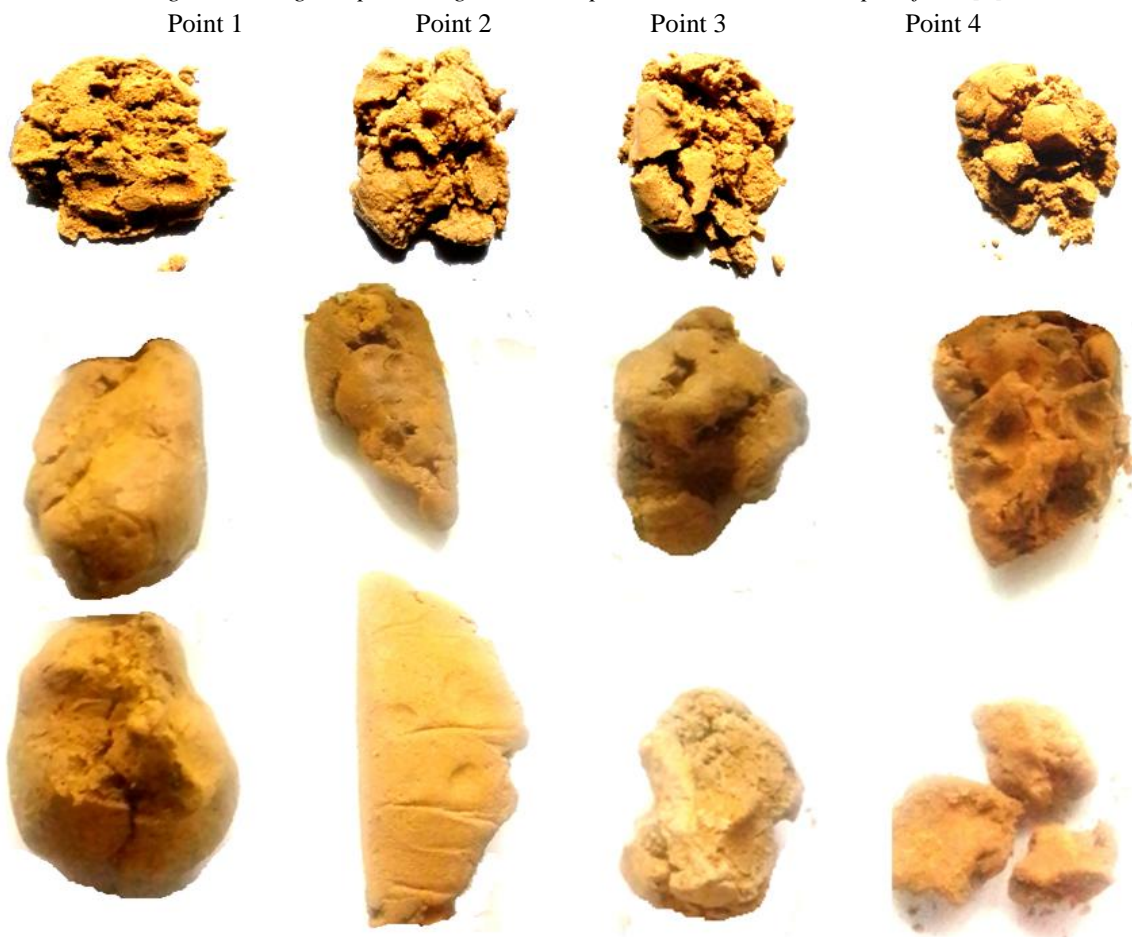


Figure 9: The Drilled soil samples in each of the sampled point

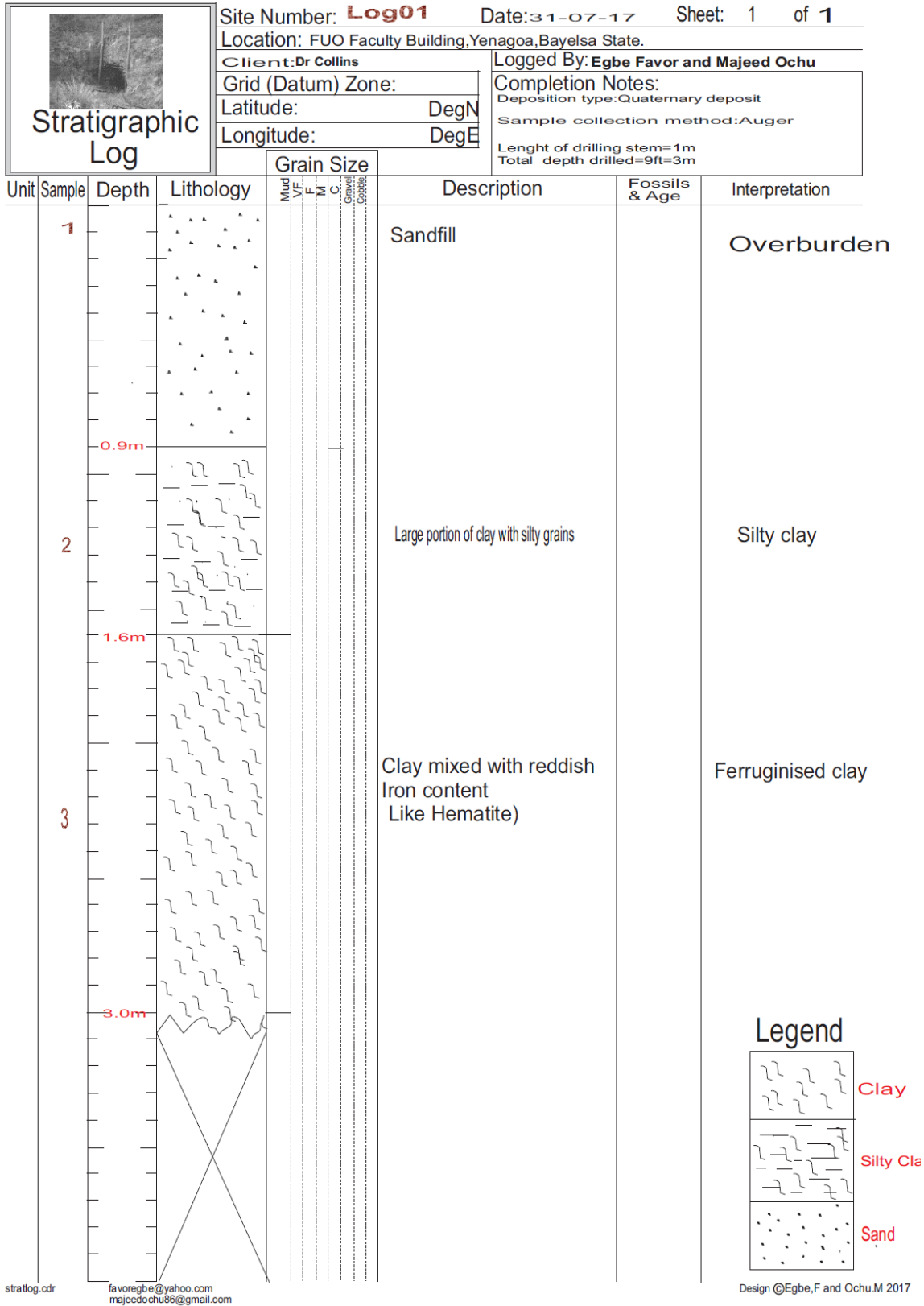


Figure 10: Stratigraphic log of point 1

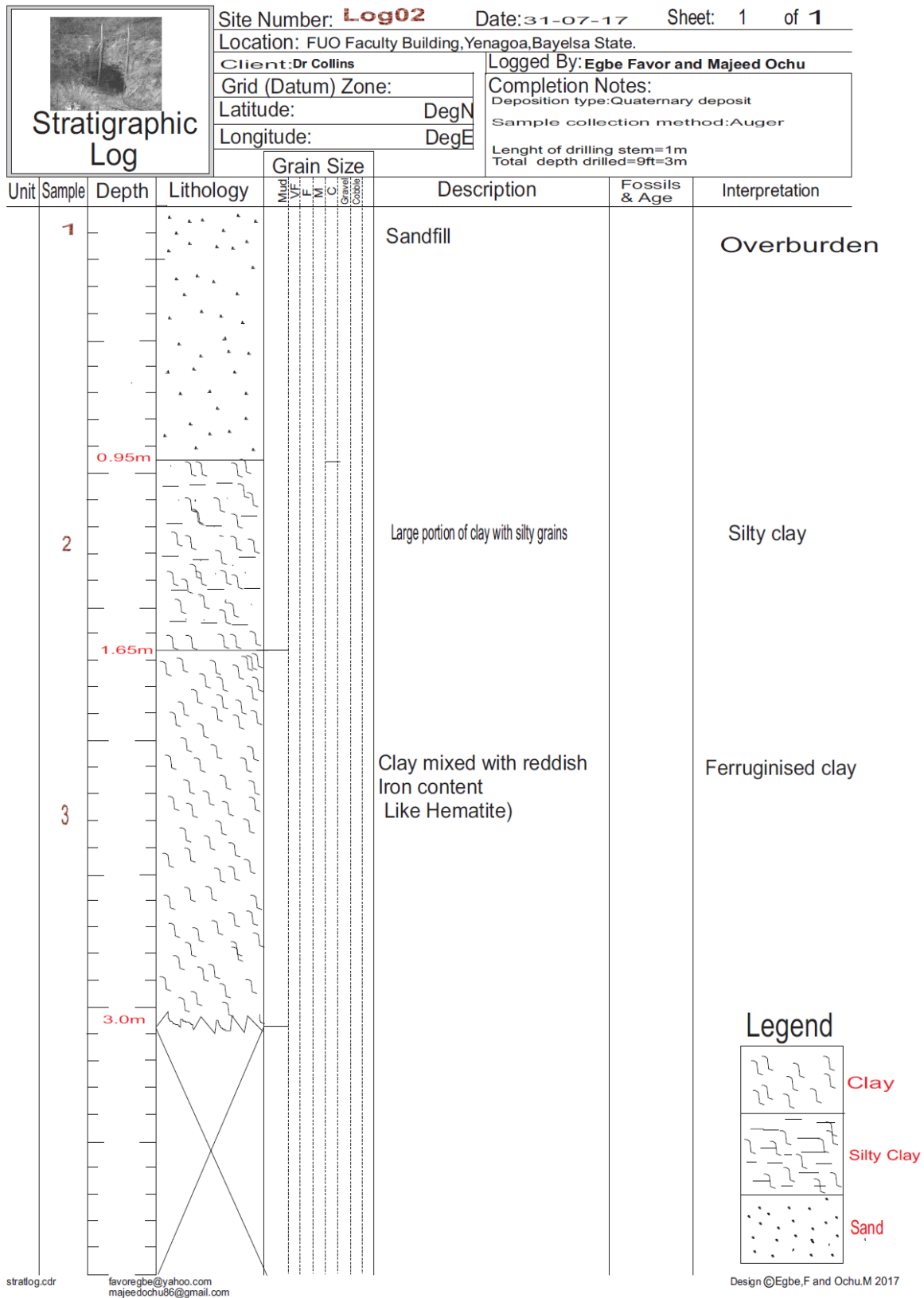


Figure 11: Stratigraphic log of point 2

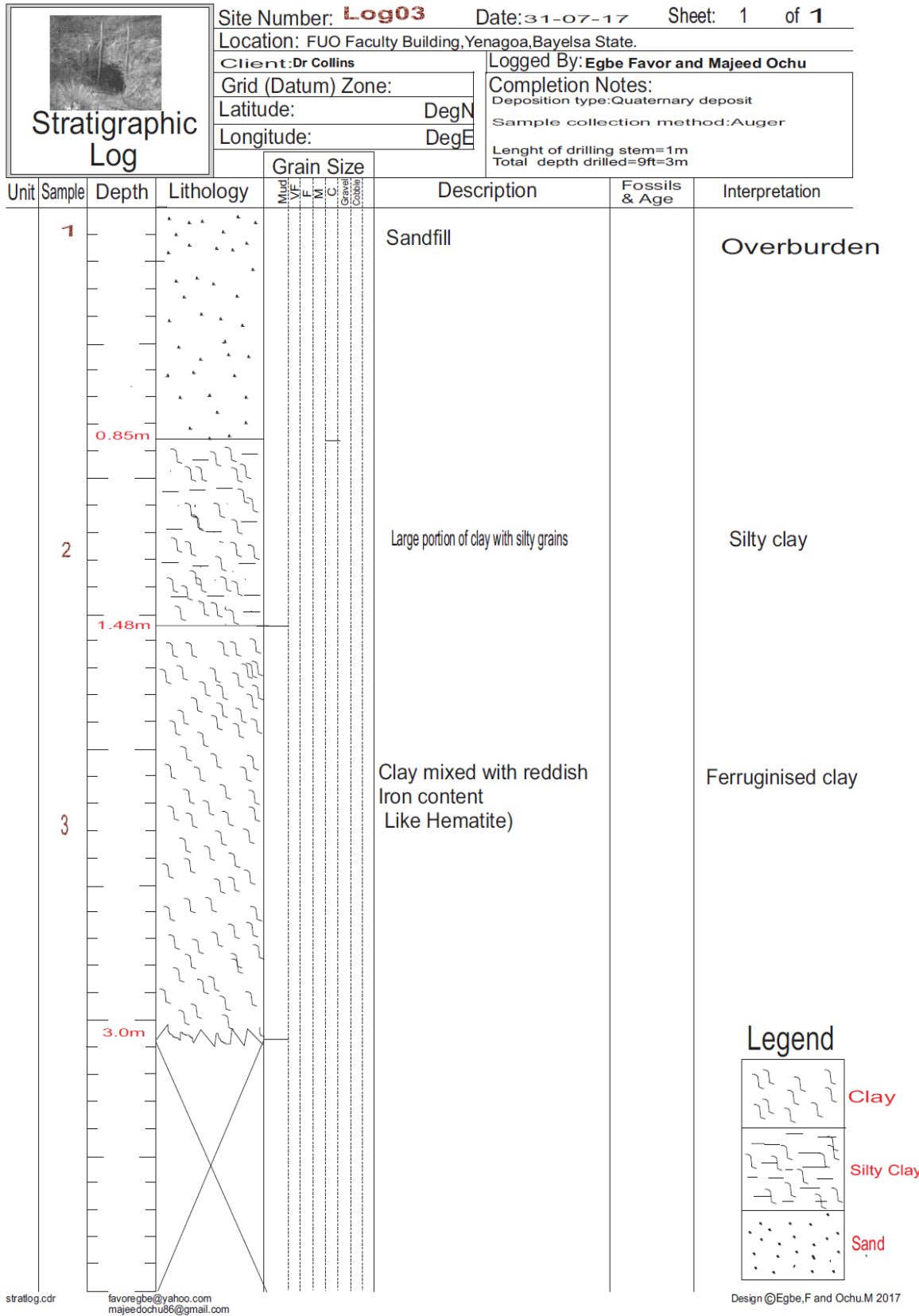


Figure 12: Stratigraphic log of point 3

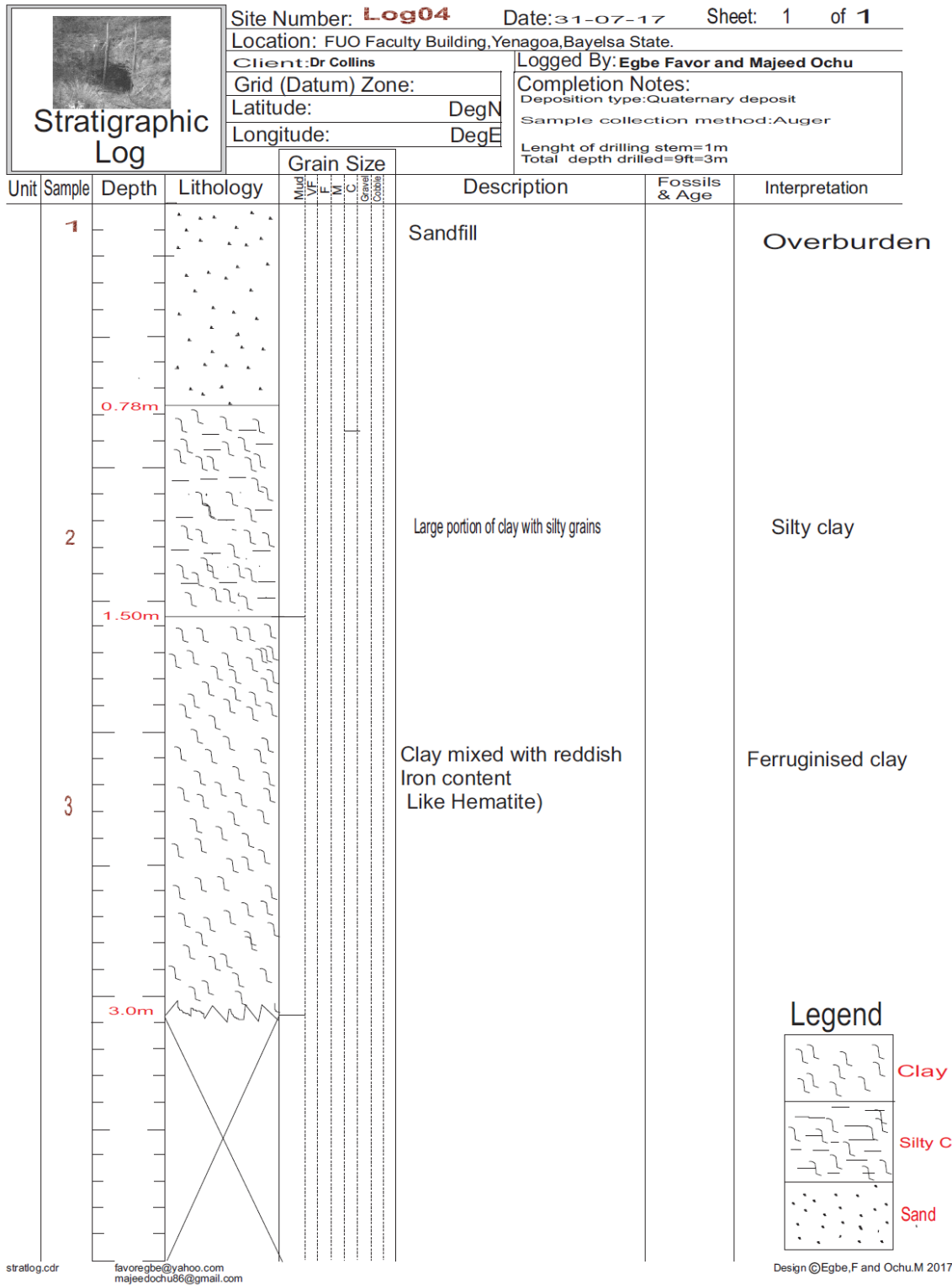


Figure 13: Stratigraphic log of point 4

Seismic refraction tomography was carried out to complement the result of resistivity tomography. The layout and the profiles length of Seismic refraction tomography compared with the resistivity profiles are exactly the same, but it penetrated down to a depth of 20 m, typical of seismic signals. The seismic tomography models were also displayed in shades of rainbow colour for easy of interpretation. The range of seismic velocity for both profiles is between 715 m/s to 1969 m/s, which also fall within the standard velocities of clay and sand.

The standard velocity for sand and clay ranges from 200 m/s to 2500 m/s (Dry Sand has a standard velocity of 200 m/s to 1000 m/s, water saturated sand 800 m/s to 2200 m/s, clay 1000 m/s to 2500 m/s after [12] and [2]). Profile 1 like the corresponding resistivity profile show a general increase of velocity with depth. The velocity of 800 m/s to 900 m/s at the surface could be attributed to that of saturated sand; this is underlain by a velocity of 1100 m/s at a depth of 1 m which could be attributed to clay. The layer of clay having a velocity of 1250 m/s to 1300 m/s extend from a depth of 1 m down to a depth of 8 m. this was interrupted by a saturated sand layer at a depth of 9 m with velocity range of 1400 m/s to 1500 m/s. This was inferred from the standard velocity and previous work after [4].

Profile 2 of seismic refraction tomography showed a great semblance with the corresponding resistivity tomography, and has the same lithological composition. The surface layer also registered a velocity range of 800 m/s to 900 m/s that can be as well attributed to the sand filling at the top layer. However, profile 2, registered disparity of seismic velocity at the surface down to an average depth of 2.5 m. The drilled point 3 and point 4 (Fig. 14) which is at a distance of 10 m and 28.5 m along the profile registered low velocities. These low velocity regions are flanked by relatively high velocity region. Low velocity signifies loose soil material occupying these regions. When the soil losses moisture these regions will contract more than the adjoining region, thereby setting up a compressional force that will produce the effects shown in figure 1 and 2. Profile 2 was also characterized with layer of clay that extends to a depth of 8m, which was interrupted by a layer of saturated sand at a depth of 9 m.

The analysis of the results of resistivity tomography, seismic refraction tomography and the lithologic logs, all pointed to the fact that the cause of the structural failure is localized movement coming from the underlying geology, rather than earth tremor or as a result of poor construction work, among others suspected causes. The results revealed that apart from the surface layer which is majorly sand, resulting from the sand filling, the survey area is predominately clay, down to an average depth of 9 m. The clay varies in types, and occasionally intermingled with sand. The results also revealed that the predominant clay layer was interrupted by a layer of saturated sand, base on the resistivity and velocity values, at an average depth of 10 m. From the analysis, it was obvious that the cause of the structural failure is due to soil material (majorly clay) having different physical properties, thereby, resulting in one contracting under the encompassing pressure of the other, setting up a compressional force that resulted to the multiple compression and breaking of the office tiles happening and the same moment.

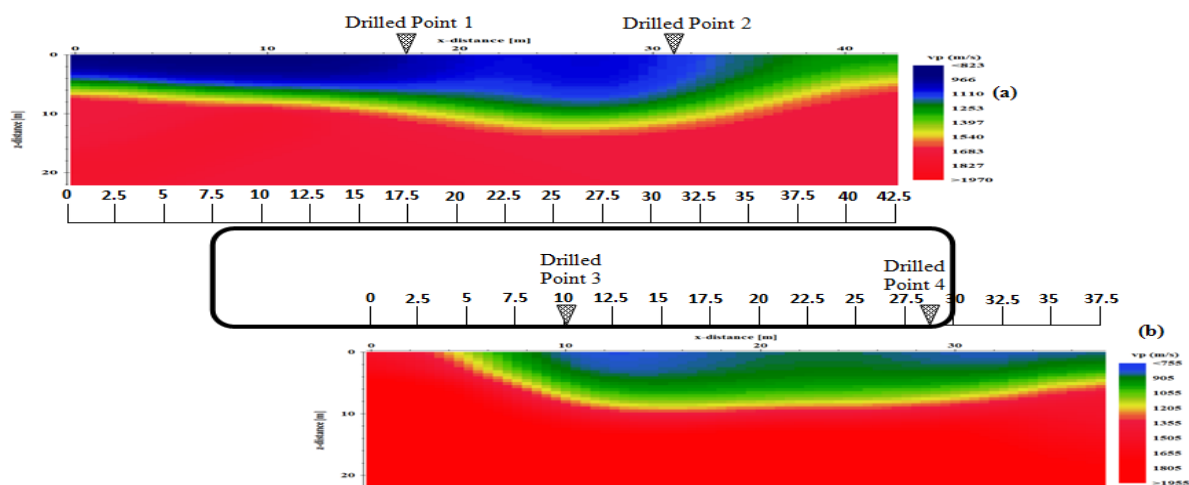


Figure 14: 2D Seismic refraction tomography models indicating profile lines around housing unit under investigation, (a) Profile 1 (b) Profile 2

It was evidence that this structural failure could have been averted, if right from the onset a comprehensive geophysical survey using integrated method was carried to identify the existing lithology and the geometry of the subsurface structure. Secondly, if the layer of clay was excavated to a uniform level before sand filling. Thirdly, figure 15 which is a 3D surface model to depict the thickness of sand filling showed that the survey region was not evenly sand fill. Point 4, in figure 15 was where the picture in figure 1 was located, and it is



apparent, it has the least thickness of the sand filling. Point 3, is where the picture in figure 2 was located, and the thickness of the sand filling is also small. If we correlate the extent of damage to the thickness of sand filling, we will discover that the point that was least sand fill experienced the highest damage compared to point 3 that was moderate damage. Point 1 and point 2 that were well sand filled have not registered any form of deformation. If the whole area under investigation properly sand fill, the impact of the uneven expansion of the clay on the structure would have been minimized.

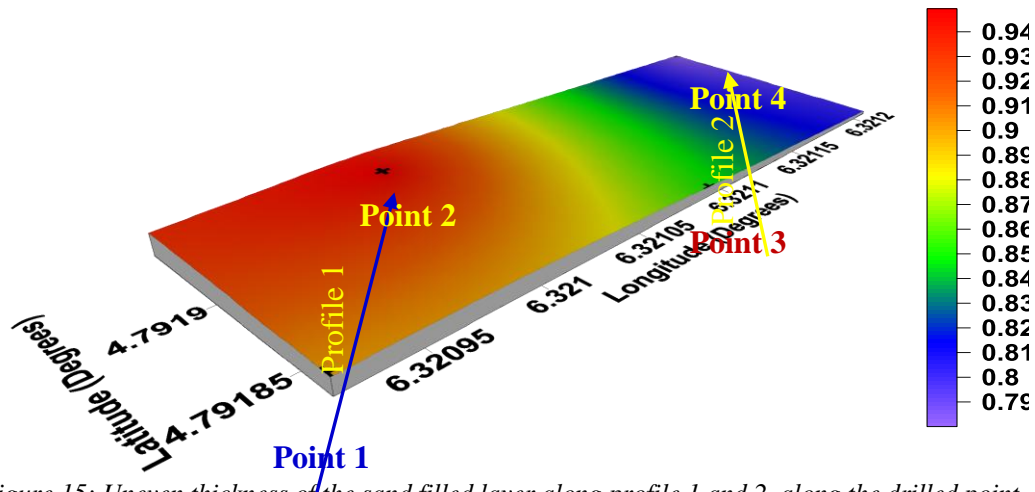


Figure 15: Uneven thickness of the sand filled layer along profile 1 and 2, along the drilled point

7. Conclusion

The results coming from the different methodology has revealed that the structure under investigation is sitting on predominately clay material of different physical property and types. It is very evident that the cause of the structural failure is not as a result of earth tremor or poor construction work during laying of the tiles, but it is due to creeping movement that was induced by the underlying geology as a result of the uneven expansion of the clay material that form the major component of the soil. In future this structural failure could be averted if adequate and comprehensive geophysical survey is carried out, to map out the geometry of the subsurface structure and identify the various lithologies in place. Also, the swampy clay layer should be uniformly excavated to at least a depth of 1m, before unvaryingly filled with sand material. In the event that the damage tiles (Fig 16) are to be replaced with new once, a gap of not less than 1.5 cm should left in between tiles, and the gap should be filled with compressible material to accommodate expansion and prevent subsequent structural failure.



Figure 16: State of the office floor after the broken tiles were removed.



Acknowledgement

I want to use this opportunity to acknowledge Isibor Kenneth Omu and Ebimi Ereyebinta Grace for their active participation during the data acquisition. Not left out in the acknowledgement are the laboratory technologists Egbe Favor and Majeed Ochu that were involve in the drilling process using handmade Augar, and for the generation of the lithologic log.

References

- [1]. Adetayo, F., (2010). Constraining Causes of Structural Failure Using Electrical Resistivity Tomography (Ert): A Case Study of Lagos, Southwestern, Nigeria. Publisher Mineral resources
- [2]. Burger, H. R., (1992). Exploration geophysics of the shallow subsurface. Norton and company, new york.
- [3]. Collins, C. C. (2015). Detail Assessment of Natural Drainage Flow Pattern in Federal University Otuoke and its Environs using Digitized Topographic Information. International Journal of Basic Science and Technology, Volume 1, Number 1, Pages 43-48.
- [4]. Collins, C. Chiemeke., Ibe, S. O., and Onyedim, G., (2016). Geophysical Investigation of the Near Surface Structure and Determination of Subsurface Lithology, Using High Resolution Seismic Method in Otuoke. International Journal of Basic Science and Technology, Volume 2, Number 1, Pages 6 – 15.
- [5]. Google Earth Imagery Map, (2017). www.google.com/earth/ (accessed 27/08/2017)
- [6]. HD Foundations, INC, (2013). What Causes Floor Cracks <https://hdfoundationrepair.com/what-causes-floor-cracks/> (accessed 28/08/2017)
- [7]. Keller G. V., Frischknecht F. C., (1996). Electrical Methods in Geophysical Prospecting. Pergamon Press, New York.
- [8]. Kogbe, C. A., (1989). The Cretaceous and Paleogene Sediments of Southern Nigeria. In: Geology of Nigeria, C.A. Kogbe, (editor), Elizabethan Press, Lagos: 311-334.
- [9]. Lee W., (2017). Seven Reasons Why Your Tile Floor Is Cracked.
- [10]. Okiongbo, K, S., and Douglas, R., (2013). Hydrogeochemical Analysis and Evaluation of Groundwater Quality in Yenagoa City and Environs, Southern Nigeria, Ife Journal of Science vol. 15, no. 2: 210.
- [11]. Osakuni, M. U., and Abam, T. K., (2004). Shallow resistivity measurement for cathodic protection of pipelines in the Niger Delta. Environmental Geology. 45: 747-752.
- [12]. Philip, K., Michael B., and Ian H., (2002). An introduction to geophysical exploration, Blackwell Science Ltd.
- [13]. Saad, R., Muztaza, M. N., Zakaria, M. T., and Saidin, M. M., (2016). Application of 2D Resistivity Imaging and Seismic Refraction Tomography to Identify Sungai Batu Sediment Depositional Origin. Journal of Geology and Geophysics, ISSN: 2381-8719,
- [14]. Short, K.C., and Stauble, A.J., (1967). Outline of the geology of the Niger Delta. Bull. AAPG. 51: 761-779.
- [15]. Type of soil and their mean value resistivity www.engineeringtoolbox.com (accessed 18/08/2017)
- [16]. Wright, J.B, Hasting, D. A., Jones, W. B., and Williams, H. R., 1985. Geology and mineral resources of West Africa, Allen and Unwin Limited, UK,: 107.

